ELSEVIER

Chemical Engineering Journal 78 (2000) 193–197

Chemical Engineering Journal

www.elsevier.com/locate/cej

Application of fractal geometry to atomization process

Zhou Weixing*, Zhao Tiejun, Wu Tao, Yu Zunhong

Institute of Clean Coal Technology, East China University of Science and Technology, P.O. Box 272, Shanghai 200237, PR China

Received 9 November 1998; received in revised form 14 January 2000; accepted 21 January 2000

Abstract

Fractal characteristics of the droplet size distribution arising in an atomization process have been studied in this paper. The fractal dimensions were measured experimentally. Simulations of droplet splitting have been carried out and the corresponding fractal dimensions have been obtained numerically. Based on the results obtained from experiments and simulations, a mathematical model of droplets splitting at uniformly distributed probability has been established.

Keywords: Fractal geometry; Atomization process; Droplet size distribution

1. Introduction

Fractal objects have been introduced into the analysis of a wide class of phenomena in physics and natural science [1]. In the field of chemical engineering, fractal geometry has been applied to describe transport, reaction, adsorption, turbulence [2], aggregation [2,3], and so on.

Kaye [4] pointed out that there exist structural and textural fractal dimensions in some natural phenomena. The structural fractal dimension D_s is defined to represent the overall topography or structure of fractals, while the textural fractal dimension D_t is used to describe the texture or fine structure of fractals.

The process of atomization is widely utilized in applying agricultural chemicals to crops, paint spraying, spray drying, food processing, cooling of nuclear cores, combustion, gasification and many other fields. Many empirical and semi-empirical models have been established to describe atomization processes. Due to the complexity of the atomization process, it is difficult to clearly describe the mechanism and also impossible to combine all the influencing factors, such as equipment dimensions, size and geometry of nozzle, physical properties of the dispersed phase and the continuous phase and operating mode, into one model. The two concepts, structural and textural dimensions, are found to be very useful in the description of atomization processes.

In this paper, the structural dimensions and textural dimensions were measured experimentally using a Malvern Laser Particle Sizer. The fractal dimensions were also calculated by numerical simulation. A mathematical derivation based on the experiment and numerical simulations is presented.

2. Experimental measurement of fractal dimensions

In order to measure the fractal dimensions, experiments have been carried out using the air–water system, with the flow chart shown in Fig. 1. The diameter of the central passage of the nozzle used was 3 mm, while that of the annular space was 23 mm. The rake angle of the nozzle was 10°. Liquid-phase water passed through the central passage at a flow rate of 0.21 m^3/h, while the continuous-phase air flow rate through the annular space is 115 N m^3/h. Malvern Laser Particle Sizer of Type 3600 [5] was utilized to measure the droplet distribution. Measurement range of the selected lens with a focal length of 1000 mm was 19.4–1879.9 μm. The measurement was carried out at the horizontal plane at a distance of 685 mm [6] from the vent of the atomizer. The measurement was repeated 50 times at the same operating mode.

A plot of the droplet number against the scale d_p on a log–log plot yields both D_s and D_t in two different scaling ranges. These two types of dimensions are shown in Fig. 2.

Fig. 2 can also be written in an analytical equation in the form

$$D_t = 0.11D_s + 0.21 \quad (1)$$

* Corresponding author. Tel.: +86-21-64252831; fax: +86-21-64250192.
E-mail address: zhwx@icct.ecust.edu.cn (Z.x. Zhou)

1385-8947/00/$ – see front matter
PII: S1385-8947(00)00130-3

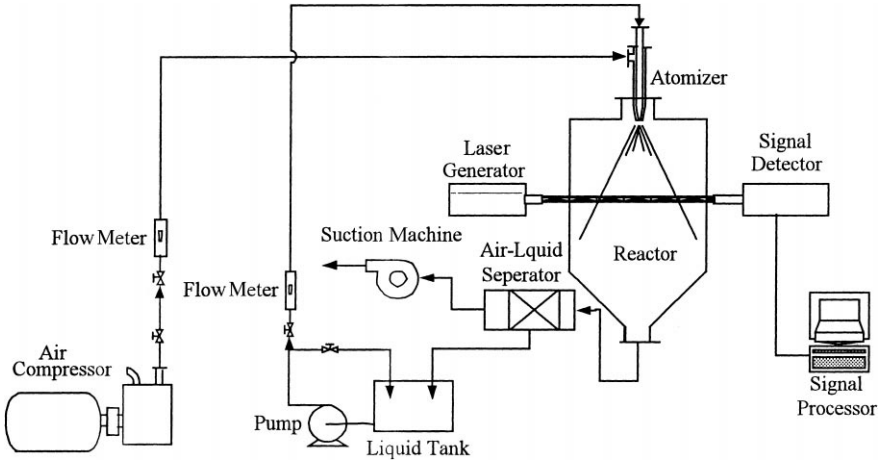

Fig. 1. Schematic diagram of the experimental apparatus.

which is a simple linear equation. The mean values of two types of fractal dimensions are expressed in Eqs. (2) and (3), respectively:

$$D_t = 0.57 \pm 0.08 \quad (2)$$

$$D_s = 3.21 \pm 0.67 \quad (3)$$

3. Numerical simulations

The Weber numbers of droplets throughout the spray regime have been estimated from the experiments. The maximum Weber number is less that 21.5. A majority of droplets in the spray had Weber numbers which were lower that the critical value of 12, indicating that these droplets lie in the vibrational break-up regime [7]. Meanwhile, the rest of the droplets had Weber numbers between 12 and 21.5 falling in the bag break-up regime. In the vibrational break-up regime, one droplet splits into two sub-droplets with the mass ratio of sub-droplet to its mother droplet being around 0.5, while in the bag break-up regime, one droplet splits into several relatively bigger sub-droplets and many smaller sub-droplets. In the case of bag break-up, we can regard the mother droplet as several *dummy* droplets.

Therefore, we represent a particle of the atomization process with two parameters, namely its age and splitting probability. Any two droplets with the same growth ages are called even-aged droplets and any two droplets with different ages are called odd-aged ones. A new concept named *generation* is introduced to denote the age of a droplet. A generation is defined to be the time gap during which a droplet may split at most into two sub-droplets, where the mass ratio of the sub-droplet to the mother droplet satisfies the same probability distribution. The growth of the first four generations of a droplet is sketched in Fig. 3 in which the splitting probability is 0.5. Therefore, we can say that the growth of a droplet has the property of statistic self-similarity.

To simulate the size distribution of an atomization process, we assume that (1) the co-effect of break-up and aggregation can be considered briefly as the effect of break-up; (2) a droplet can split at most into two sub-droplets, whose splitting probability is denoted by p; and (3) if a droplet splits into two sub-droplets, then the mass ratio, denoted by x, of a sub-droplet to the mother droplet is a random variable, and x satisfies the probabilistic distribution with the same density $f(x)$ in the open unit interval (0, 1). It is obvious that the density function $f(x)$ is symmetric about x=0.5, i.e. $f(x)$=$f(1-x)$.

Let $S(g, d_p)$ denote the set of droplets of the gth generation whose diameter is not less than d_p, and $|S(g, d_p)|$ the potential of the set $S(g, d_p)$. Following Mandelbrot's point [8], if $S(g, d_0)$ is a fractal set, then its distribution takes the form of

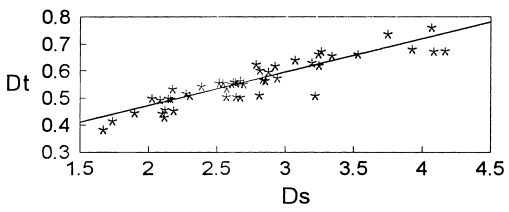

Fig. 2. Relationship between D_t and D_s.

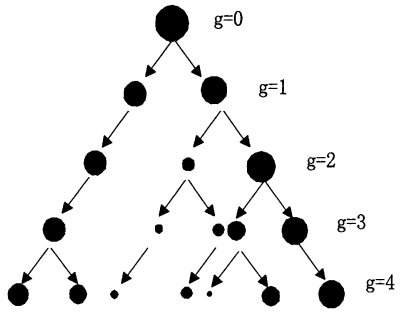

Fig. 3. Growth tree of a droplet: g=0, 1, 2, 3, 4; p=0.5.

$$|S(g, d_p)| = A(g)d_p^{-D} \tag{4}$$

in which $A(g)$ is independent of resolution d_p which is not less than d_0.

To prove that $|S(g, d_p)|$ is a fractal set, simulations in the case wherein $f(x)$ is the density of uniform distribution are performed. A so-called Richardson–Mandelbrot plot [9] which is a plot of $\log(|S(g, d_p)|)$ against d_p on a log–log plot yields a structural fractal dimension and a textural fractal dimension at two different scaling ranges, respectively.

The growth of 10 primary droplets has been simulated which has been repeated 50 times. The pseudo-random numbers are generated using the pseudo-random number generator of MATLAB 5.0, and all these simulations can be reduplicated.

We have calculated the structural fractal dimensions and the textural fractal dimensions of even-aged droplets with the generation number g from 19 to 30 whose step size is 1 and the splitting probability p from 0.22 to 0.38 whose step size is 0.02.

Plots of D_t of the even-aged droplets against p show perfect linear relationships, all of whose correlation coefficients are greater than 0.99. The fitted multiple regression equation is obtained as follows:

$$D_t = (0.322\,g - 4.964)\,p - 0.045\,g + 0.612 \tag{5}$$

The relative errors between fitted values and simulated values are mostly less than 10%. From Eq. (5), it can be seen that D_t increases with increasing g and p, which also shows that the fine structure becomes more and more obvious and moves to the smaller scale range with development of the jet flow and increase in the splitting probability.

Likewise, the fitted multiple regression equation of D_s against g and p is obtained as follows:

$$D_s = (0.250\,g - 7.836)\,p - 0.104\,g + 6.264 \tag{6}$$

The relative errors between fitted values and simulated values are mostly less than 9%. From Eq. (6), it can be seen that D_s decreases with increasing g and p, which also shows that the fine structure moves to the smaller scale range with development of the jet flow and increase in the splitting probability. Moreover, the average of all D_s's gives

$$D_s = 3.21 \pm 0.19 \tag{7}$$

which can also be acceptable.

4. Mathematical model

Consider the set $S(g, d_0)$, given an arbitrary element s of $S(g, 0)$ with the diameter d_g. If s splits into two sub-droplets denoted by s_1 and s_2, there exist three cases:

1. If $d_g < d_0$, then s does not belong to $S(g, d_0)$, and so also s_1 and s_2.

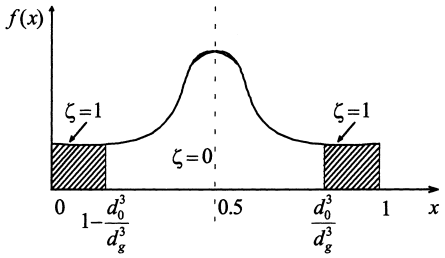

Fig. 4. Sketch for Case 2.

2. If $d_0 \le d_g < \sqrt[3]{2}d_0$, then $s \in S(g, d_0)$, and there is at least one sub-droplet which does not belong to $S(g+1, d_0)$. If $s_i \notin S(g+1, d_0)$ ($i=1$ and $i=2$), it follows that

$$d_{g+1}^3 \le d_0^3 \quad \text{and} \quad d_g^3 - d_{g+1}^3 \le d_0^3$$

$$1 - \frac{d_0^3}{d_g^3} \le \frac{d_{g+1}^3}{d_g^3} \le \frac{d_0^3}{d_g^3}$$

Hence, if $x \in [1 - (d_0^3/d_g^3), d_0^3/d_g^3]$, then both the sub-droplets do not belong to $S(g+1, d_0)$, as shown in Fig. 4.

3. If $\sqrt[3]{2}d_0 \le d_g$, then $s \in S(g, d_0)$, and there is at the most one sub-droplet which does not belong to $S(g+1, d_0)$. If $s_i \in S(g+1, d_0)$ ($i=1$ and $i=2$), it follows that

$$d_0^3 \le d_{g+1}^3 \quad \text{and} \quad d_0^3 \le d_g^3 - d_{g+1}^3$$

$$\frac{d_0^3}{d_g^3} \le \frac{d_{g+1}^3}{d_g^3} \le 1 - \frac{d_0^3}{d_g^3}$$

Hence, if $x \in [d_0^3/d_g^3, 1 - (d_0^3/d_g^3)]$, then both the sub-droplets belong to $S(g+1, d_0)$, as shown in Fig. 5.

It is obvious that the number of sub-droplets generated by any arbitrary mother droplet is also a random variable. If we denote this random variable as ζ, then the possible value of ζ is 0, 1, and 2, as shown in Figs. 4 and 5. Therefore, the expectation of ζ in the second case given above is calculated to be

$$E(\zeta) = 1 - p + \int_0^{1-(d_0^3/d_g^3)} f(x)\,\mathrm{d}x + \int_{d_0^3/d_g^3}^1 f(x)\,\mathrm{d}x$$

$$= 1 - p + 2\int_0^{1-(d_0^3/d_g^3)} f(x)\,\mathrm{d}x \tag{a}$$

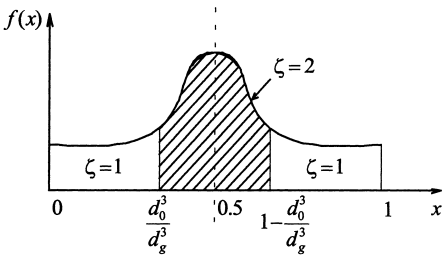

Fig. 5. Sketch for Case 3.

and in the third case, it is calculated to be

$$E(\zeta) = 1 - p + \int_0^{d_0^3/d_g^3} f(x)\,\mathrm{d}x + \int_{d_0^3/d_g^3}^{1-(d_0^3/d_g^3)} 2f(x)\,\mathrm{d}x + \int_{1-(d_0^3/d_g^3)}^{1} f(x)\,\mathrm{d}x = 1 - p + 2\int_0^{1-(d_0^3/d_g^3)} f(x)\,\mathrm{d}x \quad \text{(b)}$$

According to Eqs. (a) and (b), it follows that, for any s in $S(g, d_0)$ with a diameter d_p, the expectation of ζ is

$$E(\zeta) = 1 - p + 2\int_0^{1-(d_0^3/d_p^3)} f(x)\,\mathrm{d}x \tag{8}$$

For the gth generation droplets, the number of the given s in the scale interval $[d_p, d_p+\mathrm{d}d_p]$ is $-\mathrm{d}|S(g, d_p)|$. Hence, there are $-E(\zeta)\cdot\mathrm{d}|S(g, d_p)|$ droplets generated by $|S(g, d_p)|$ mother droplets belonging to $|S(g+1, d_p)|$. Therefore, it follows that

$$|S(g+1, d_0)| = \int_{d_0}^{\infty} -E(\zeta)\frac{\mathrm{d}|S(g, d_p)|}{\mathrm{d}d_p}\mathrm{d}d_p \tag{9}$$

Substitution of Eq. (8) into Eq. (9) gives

$$|S(g+1, d_0)| = (1-p)|S(g, d_0)| - 2\int_{d_0}^{\infty} \times \left[\int_0^{1-(d_0^3/d_p^3)} f(x)\,\mathrm{d}x\right] \frac{\mathrm{d}|S(g, d_p)|}{\mathrm{d}d_p}\mathrm{d}d_p \tag{10}$$

where the identity $|S(g, \infty)|\equiv 0$ is used.

If $f(x)$ is the density of a uniformly distributed function in the open unit interval (0, 1), according to the normalizing condition, we have

$$\int_0^1 f(x)\,\mathrm{d}x = p$$

where $f(x)$ is a constant in (0, 1). It follows that $f(x)=p$, where $x\in(0, 1)$. Therefore, we obtain

$$|S(g+1, d_0)| = (1+p)|S(g, d_0)| + 2p\int_{d_0}^{\infty} \frac{d_0^3}{d_p^3}\frac{\mathrm{d}|S(g, d_p)|}{\mathrm{d}d_p}\mathrm{d}d_p \tag{11}$$

Eq. (11) is the recursion formula of $|S(g, d_p)|$ about the generation number g. Both simulations of physical model and experimental measurements verify that the droplets' set $S(g, d_p)$ is a fractal set, namely, Eq. (4) which is correct for those generation numbers which are large enough. Substitution of Eq. (4) into Eq. (11) gives

$$|S(g+1, d_0)| = \left(1 + p - \frac{2Dp}{3+D}\right) A(g) d_0^{-D} = \left(1 + p - \frac{2Dp}{3+D}\right) |S(g, d_0)| \tag{12}$$

Let $1+p-(2Dp/(3+D))=A(g+1)$; then, we have

$$|S(g+1, d_0)| = A(g+1)d_0^{-D} \tag{13}$$

which has the same form as Eq. (4).

5. Discussion

5.1. Critical fractal dimension and its application

From Eq. (12), one can see that there exists a critical fractal dimension $D_c=3$ for the case of uniformly distributed probability.

If $D>D_c$, then $|S(g+1, d_p)|<|S(g, d_p)|$ and the number of droplets decreases with increasing g in the corresponding scaling range.

If $D=D_c$, then $|S(g+1, d_p)|=|S(g, d_p)|$ and the number of droplets is constant over different g in the corresponding scaling range.

If $D<D_c$, then $|S(g+1, d_p)|>|S(g, d_p)|$ and the number of droplets increases with increasing g in the corresponding scaling range.

Let $M(g, d_p)$ denote the total mass of the set $S(g, d_p)$. Consider the case that $D>D_c$. We have

$$M(g, d_p) = \int_{s\in S(g,d_p)} -\rho\left(\frac{1}{6}\pi d_p^3\right)\mathrm{d}|S(g, d_p)| = \int_{d_p}^{\infty} \rho\left(\frac{1}{6}\pi d_p^3\right) A(g) D d_p^{-D-1}\mathrm{d}d_p = \frac{\rho\pi}{6}\frac{D}{D-3}A(g)d_p^{3-D} \tag{14}$$

which shows that the mass distribution also has fractal characteristics if the fractal dimension is greater than the critical fractal dimension D_c.

5.2. Structural fractal dimensions of odd-aged droplets

According to the mathematical model, all different-generation droplets have the same structural fractal dimension if the generation number is large enough. Eq. (12) can also be expressed in the form

$$|S(g+n, d_p)| = \left(1 + p - \frac{2Dp}{3+D}\right)^n |S(g, d_p)| \tag{15}$$

Simulations make it possible to calculate the fractal dimension of odd-aged droplets according to Eq. (15). The computed fractal dimensions D are listed in Table 1. It is obvious that these fractal dimensions are structural fractal dimensions and the mean D_s is coincidental with Eq. (3). These computations of D_s also test and verify the derivation results of the mathematical model.

Now, consider the structural fractal dimensions expressed in formulae (3) and (7), and in Table 1. We find that they are all coincidental with each other. We also find that the textural

Table 1
Structural fractal dimensions of odd-aged droplets

	Splitting probability								Mean
	0.20	0.22	0.24	0.26	0.28	0.3	0.32	0.34	
Resolution	0.20	0.20	0.15	0.15	0.15	0.10	0.25	0.10	0.15
Fractal dimension	3.31	3.69	3.19	3.43	3.57	2.79	3.00	3.23	3.28
Standard deviation	0.38	0.50	0.28	0.33	0.34	0.22	0.22	0.25	0.27

fractal dimension shown in formula (2) is not contradictory to that in formula (5).

5.3. Approximation of overall droplets distribution

Consider the overall atomization process. In order to obtain the droplet size distribution, we assume that all the sets $S(g, d_p)$ with any arbitrary generation number g are fractal sets, i.e. Eq. (4) holds. For some proper fixed d_p, summation of all $|S(g, d_p)|$ about g from 1 to some g gives

$$\sum_{i=1}^{g}|S(i, d_p)| = \sum_{i=1}^{g}A(i)d_p^{-D} \tag{16}$$

Since all $A(i)$ is independent of d_p and D is a constant according to the hypothesis, we can draw a conclusion that the overall distribution approximately takes the form

$$N(d_p) = Ad_p^{-D} \tag{17}$$

where $N(d_p) = \sum_{i=1}^{g}|S(i, d_p)|$ and $A = \sum_{i=1}^{g}A(i)$. Hence, we can take it for granted that, in a proper scaling range, Eq. (17) gives a perfect approximation of the overall atomization size distribution as long as we take a large enough number of g.

6. Conclusions

We have introduced a new concept, the *generation*, to describe an atomization process. Both simulations and experiments show that the droplet size distribution occurring in a nozzle atomization process has the fractal characteristics in the proper scaling range, which is represented by D_s at the larger scale and D_t at the small scale. Atomization processes can be modeled by the growth of droplets at a probabilistically uniform distribution. We have proved that all droplets at different generations have the same structural fractal dimension if and only if the generation number is large enough based on the results of simulations and experiments.

A so-called critical fractal dimension, whose value is 3, is discovered to specify whether the atomization process is an aggregation process or a break-up process and to distinguish between the structural and textural fractal dimensions. Moreover, a recursion formula of the droplet number between the different generations is obtained.

It is necessary to point out that the physical and mathematical models can also be applied to other growth processes such as the fracture of rock. It is, however, necessary to verify the trueness of Eq. (4) by experiments.

Acknowledgements

We are grateful to Dr. E.H. Cao for useful suggestions. This research was supported by the National Development Programming of Key and Fundamental Researches of China (No. G1999022103).

References

[1] B.B. Mandelbrot, The Fractal Geometry of Nature, Freeman, New York, 1982.
[2] M. Giona, G. Biardi, Fractals and Chaos in Chemical Engineering, World Scientific, Singapore, 1996.
[3] L. Pietronero, E. Tosatti, Fractals in Physics, Elsevier, New York, 1986, pp. 205–283.
[4] B.H. Kaye, A Random Walk Through Fractal Dimensions, VCH, New York, 1989, pp. 25–31.
[5] A.H. Lefebvre, Atomization and Sprays, HPC, New York, 1989, pp. 397–400.
[6] M.J. Mccauchy, N.A. Molley, Review of stability of liquid jets and influence of nozzle design, J. Chem. Eng. 17 (1) (1974) 1–20.
[7] M. Pilch, C.A. Erdman, Int. J. Multiphase Flow 13 (1987) 741–753.
[8] B.B. Mandelbrot, The Fractal Geometry of Nature, Freeman, New York, 1982, pp. 116–130.
[9] R. Creutzburg, E. Ivanov, in: H.O. Peitgen, J.M. Henriques, L.F. Penedo (Eds.), Increasing the Accuracy of Fractal Dimension Computed from the Richard–Mandelbrot-Plot. Fractals in the Fundamental and Applied Science, Elsevier, New York, 1991, pp. 95–100.